

# 3D segmentation of the tracheobronchial tree using multiscale morphology enhancement filter

Samah Bouzidi  
Univ. Bordeaux, LaBRI,  
UMR 5800, F-33400  
Talence  
ReGIM, University of  
Sfax, Tunisia  
sbouzidi@labri.fr

Fabien Baldacci  
Univ. Bordeaux, LaBRI,  
UMR 5800, F-33400  
Talence  
fabien.baldacci@labri.fr

Chokri Ben Amar  
Research Group in  
Intelligent  
Machines(ReGIM),  
University of Sfax ,  
Tunisia  
chokri.benamar@ieee.org

Pascal Desbarats  
Univ. Bordeaux, LaBRI,  
UMR 5800, F-33400  
Talence  
pascal.desbarats@labri.fr

## ABSTRACT

In this article we present a new region growing algorithm for airway segmentation based on multiscale black top-hat enhancement filter. Lung airways are tubular structures that display specific characteristics, such as highly variable intensity levels within the lumen and proximity to vessels. The proposed airways enhancement filter aims to separate airways from adjacent lung parenchyma and vessel. Based on the filter output, the region growing is performed in order to delineate the airways and then to reconstruct the tracheobronchial tree. The proposed method has been applied on various CT scans. In this paper, an experimental comparison study between our filter and the "gold standard" filters used to enhance tubular structures (Frangi, Sato and Krissian filters) followed by a region growing process is performed on data from the *VESSEL12* challenge framework. Our approach outperforms the other considered methods in terms of retrieved bronchi and computing time.

## Keywords

bronchial segmentation, enhancement filter, lung, CT chest scan.

## 1 INTRODUCTION

Visualisation and analysis of human tracheobronchial tree (TBT) is crucial for many clinical procedures. The assessments of the airways tree structure and the monitoring of lung interventions requires a good knowledge of the airway morphometry such as airway wall thickness and lumen diameter. With the introduction of Computed Tomography (CT) scanning into the non-invasively assessing of lung abnormalities, a 3D extraction and visualisation of the TBT has become more important. Anatomically, the tracheobronchial tree consists of a network of hollow branching tubes that enable airflow to go into the lungs through the main airways, the trachea. Boyden [3] proposed to decompose the TBT to 23 generations where generation zero corresponds to the trachea, the 3<sup>rd</sup> generation to the segmental bronchus, the 4<sup>th</sup> to the subsegmental bronchus and the 23<sup>rd</sup> generation corresponds to terminal bronchioles. As the tree penetrates deeper into the lungs, the airways size decrease, e.g the 7<sup>th</sup> branching generation can have diameters in the *mm* range. This complex branching structure makes its manual extraction

process tedious, time consuming and changing across image analysts. A large amount of airways analysis has been reported in the literature. Most of proposed methods of airways tree segmentation are based on the extraction of the airway lumen which appears in CT chest scan as a dark tube surrounded by a bright airway wall. Based on that assumption, numerous approaches [4, 12, 17, 18] used region growing process to segment the tree. Starting from a seedpoint within the trachea, voxels are added to the process if its X-ray density belong to the lumen density range. However, intensity based region growing deals with many difficulties and often leads to leakage into the lung parenchyma. First, there is no standard lumen intensity range since CT scans may be acquired under different scanning conditions and/or depict different diseases. Second, as noise and partial volume effects decrease the contrast between the air and the surrounding tissue then the whole lung can be added to the growing region. Last but not least, growth can also be interrupted earlier in case of lung disease (e.g., emphysema). The segmentation process is blocked in distal bronchial generation. Despite

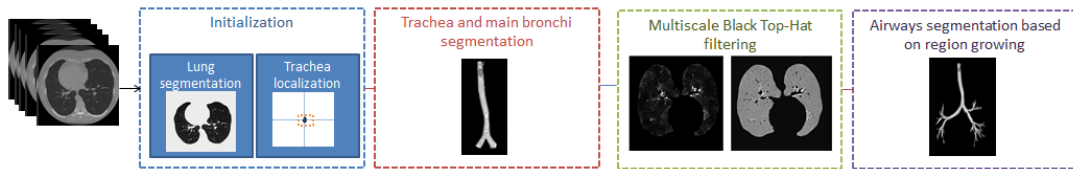


Figure 1: Overview of the proposed method.

of these limitations and due to its simple implementation, region growing is still the most popular approach to segment airways tree. To overcome their problems, several strategies have been proposed to improve region growing results.

In this paper, region growing are performed twice. First, an intensity based region growing is employed to segment trachea and main bronchi. Then, the input volume is enhanced using the multiscale Black Top-Hat filter. Therefore, small airways wall becomes more distinguish from background. Thereafter, the second region growing is performed on the processed volume to extract the TBT and prevent leakage. The content of this paper may be summarized as follows. In section 2, an overview of existing airways segmentation approaches are presented. In section 3, the proposed method is explained in detail. Section 4 presents the experimental results. Finally, conclusions and perspectives are drawn in section 5.

## 2 RELATED WORKS

A lots of efforts have been made to prevent region growing from leaking into the lung parenchyma by adjusting the growing criterion. Mori et al. [13] proposed explosion-controlled region growing algorithm that updates iteratively the intensity threshold until parenchymal leakage (explosion) is detected. Fabijanska [4] used two passes of 3D seeded region growing where the second one is guided by a morphological gradient information that allows to locally identify airways region and prevents the process from leakage. Weinheimer et al. [19] employed an adaptive region growing approach constrained by airways lumen and wall intensities thresholds and performed in axial, coronal, and sagittal plane. Similarly to Mori’s method [13], Lee et al. [11] proposed an adaptive region growing method applied within localized cylindrical volumes in order to control the segmentation process. Other works address the RG leakage problem by filtering the image before performing the tree segmentation. In that approach, tubular enhancement filters based on hessian matrix analysis [12, 17] and mathematical morphology operations [1, 14, 9] are used to isolate candidate airway locations. In the work of Lo et al. [12] the growing criterion is based on an airways classifier and vessel orientation similarity that use hessian matrix analysis. First, Hessian eigenvalues analysis are employed twice to differentiate airways and vessel voxels. From obtained

vessel voxel, Hessian eigenvector analysis is performed to define neighboring airways orientation. Aykac et al [1] and Pisupati et al. [14] used grayscale mathematical morphology to identify candidate airways on 2-D CT slices. The grayscale reconstruction is performed using different sized structure elements (SE) in order to detect airways over a wide range of sizes. Airways tree is then reconstructed using slice by slice region growing. Similarly, Irving et al. [9] applied multiscale morphological filtering in the axial, sagittal and coronal planes of the volume. After thresholding the enhanced volume, airways are segmented using 3D bounded space dilation region growing.

## 3 MATERIAL AND METHODS

The proposed algorithm consists of four steps and the whole process can be seen in the Figure 1, The input is a 3-D X-ray CT image volume that displays all the structures in the patient’s chest, including lungs. The algorithm starts by extracting lungs. The obtained volume is firstly used to perform the region growing and segment main bronchii and is secondly improved by the multiscale Black Top-Hat filter in order to perform the second region growing that adds small bronchi.

### 3.1 Lung segmentation

Lungs segmentation is performed using a simplified version of Hu et al. [8] and Heuberger et al. [7] algorithms. First of all, the input image is thresholded to separate low-intensity pixels (lung and surrounding air voxels) from high-intensity voxels (hard and soft tissues voxels), the obtained image is illustrated in Figure 2.(b). Then the surrounding air, which is the set of pixels connected to image borders, is identified and removed from the lung volume (see Figure 2.(c)). After that, the lung mask is created by cleaning the interior of lung from noise and airways using morphological closing operation. Finally, the obtained mask is applied on the initial volume to extract lungs and trachea.

### 3.2 Main bronchi segmentation

#### 3.2.1 Trachea localization

The trachea is localised using the output of the lung segmentation algorithm. The slices are orientated using the DICOM header information (header first/feet first flag) and we search the first slice that contains voxels assigned to the lung region. An horizontal pass through

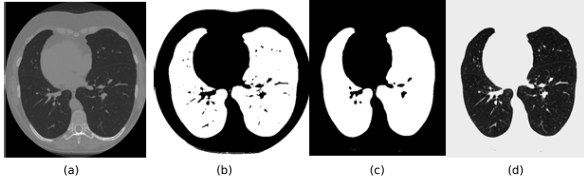


Figure 2: Lung segmentation steps: (a) original, (b) thresholding, (c) background removal and mask creation, (d) lung extraction.

the extracted slice is performed in order to extract trachea voxels as shown in Figure 3. The center of the trachea is the pixel located in the middle of the trachea voxels set. We use this voxel as the seed point for the following region growing process.

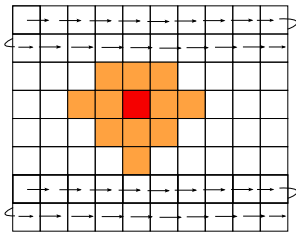


Figure 3: Trachea localization. Trachea pixels set is marked in yellow and trachea seed point is marked in red.

### 3.2.2 First region growing process

After the seed voxel of the region growing algorithm is determined, all their 26-connected neighbours are added to the growing process in order to initialize the growing criterion. We define this criterion as the range between the minimum intensity value of a CT image and the maximum intensity value of added voxels. After that, the 3D intensity based region growing is performed and the upper bound of the growing criterion is adjusted as the initialization step.

The algorithm is stopped when the number of bifurcation is equal to two, which mean that trachea and one of the main bronchi are extracted. The second one will be fully extracted by the second region growing process.

### 3.3 Multiscale Black Top-Hat filtering

As stated in section 2, graylevel morphological techniques have been widely used to enhance the airways in CT slices. In our case, we use a Black Top-Hat transform (BTH) [6] embedded in a multiscale framework to identify the airways location. In other words, the proposed multiscale Black Top-Hat algorithm integrates the idea of iteratively increasing the structuring element (SE) size to capture smallest and largest bronchi in the lung.

We define the multiscale structuring elements set  $\{B_1, B_2, B_3, \dots, B_n\}$  as a set of binary diamond SE with

increasing size where  $B_i$  is the result of  $i^{th}$  dilation as follows:

$$B^i = B \oplus B \oplus \dots \oplus B \quad (1)$$

Airways extracted at the  $i^{th}$  scale by the BTH can be expressed as follows:

$$A_i = I \bullet B^i - I \quad (2)$$

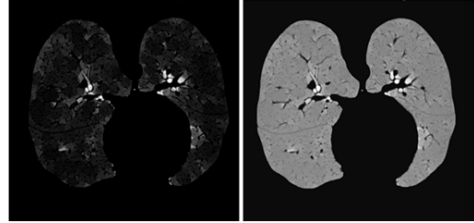


Figure 4: Airways highlighted using the Black Top-Hat transform. Left: the multiscale response of the filter applied in axial slice. Right: its corresponding image difference.

For each slice, the corresponding BTH enhanced is obtained after combining the airways location extracted at each scale (see eq 3). Then, the union of this series of images is taken to form the final Enhanced Airways volume (EA) as described in eq 4.

$$A = \bigcup_i A_i \quad (3)$$

$$EA = \bigcup_z A \quad (4)$$

A grayscale difference volume  $D$  is then computed to distinguish more airway locations from lung parenchyma and vessels. Figure 4 illustrates the application of the BTH on the input image and its corresponding image difference in the volume  $D$ .

### 3.4 Second region growing

The second 3D region growing aims to add lung bronchi to the volume defined in 3.2.2. The growing process is performed on the enhanced BTH volume obtained from the previous step. We define the seeds points as the set of points obtained after the first segmentation. Voxels are added to the final volume if their intensities and the intensities of all their neighbours belong to the ranges of enhanced airway lumen. The range was chosen experimentally.

## 4 RESULTS

In this section, our method's efficiency is evaluated by comparison to a rough region growing with manually selected threshold results and to state-of-the-art

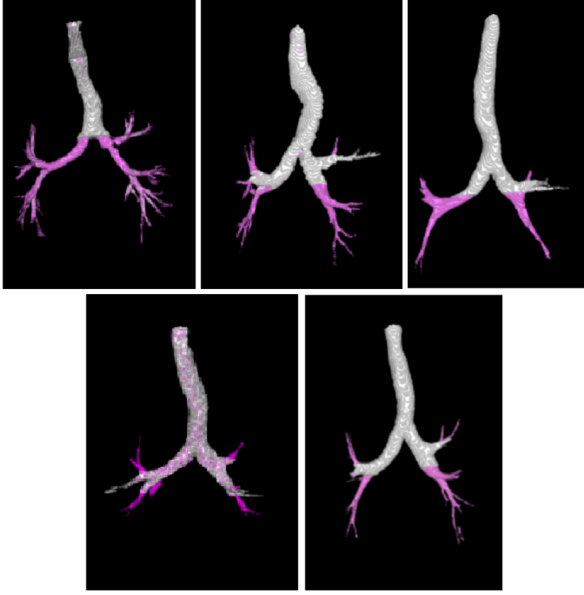


Figure 5: Segmentation results of airway tree segmentation using proposed method and the raw region growing. Airways marked in white are those extracted by the raw region growing. Airways segmented during the proposed algorithm are assigned with pink colour.

Hessian-based vessel enhancement filters. The first filter is the "gold-standard" Frangi vesselness filter [5]. The second is the Sato's line filter [16] and the third is the medialness Hessian-based vesselness filter derived from the work of Krissian et al. [10]. All filters are presented in section 4.2.2. All computations were performed on an intel-Xeon E3-1200 @ 3.60GHz, 16GB RAM, Ubuntu Linux 64 bit.

#### 4.1 Clinical data

We have first assessed qualitatively our method using various CT chest scan. Then, we have used data from the *VESSEL12* challenge (<http://vessel12.grand-challenge.org/>) for the quantitative analysis of airway tree segments of each method. The evaluation database included five pairs of anonymized MSCT cases acquired using several CT scanners and protocols [15]. Table. 1 presents the characteristics of each scan.

#### 4.2 Segmentation results evaluation

Results of applying proposed algorithm to the first five *VESSEL12* CT data sets are illustrated in Figure 5. In the context of airways segmentation, the assessment of segmentation results is a tedious task if the gold standard isn't provided. A manual segmentation can be a good alternative except however the operation is very time consuming and requires expert's skills. In our case, as the gold standard isn't available, we compare our results with the TBT trees obtained when the data is enhanced or not.

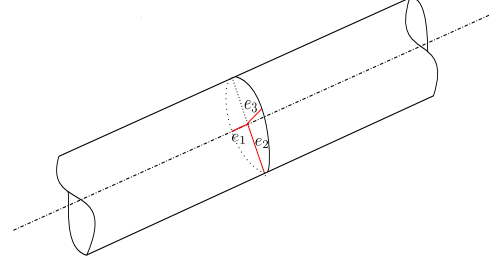


Figure 6: The eigenvalues  $e_2$  and  $e_3$  of the Hessian matrix define the principal curvature of the tube [2].

##### 4.2.1 Proposed method vs raw RG

We first compare the performance of our algorithm to the rough region growing (RRG) algorithm. Intensities range parameters of the later are selected for each scan manually in order to avoid leakage. As illustrated in Figure 5.(a) our algorithm successfully extend from the first generation which is the final generation obtained by the RRG algorithm to the sixth generation. The added bronchi are presented in pink while the branches detected by both algorithms are shown in white.

##### 4.2.2 Proposed method vs Hessian based enhancement filters

We first present in what follow the theory behind the three enhancement filters used for comparison propose.

**Frangi line filter.** Frangi et al. [5] perform a Hessian eigenvalue analysis to enhance voxel within tubular structures (vessels, airways...). Based on the information that dark tubular structures have two positive larger eigenvalues ( $e_3 > 0$  and  $e_2 > 0$ ) and the third eigenvalue being close to zero ( $e_1 \approx 0$ ). The proposed line filter is defined as:

$$T(x) = \begin{cases} ((1 - \exp(-\frac{R_A^2}{2\alpha^2}))\exp(-\frac{R_B^2}{2\beta^2}))(1 - \exp(-\frac{S^2}{2\gamma^2})) & 0, e_3 < 0 \text{ and } e_2 < 0 \\ 0, e_3 < 0 \text{ and } e_2 < 0 \end{cases} \quad (5)$$

with  $R_A = |\frac{e_2}{e_3}|$ ,  $R_B = \frac{|e_1|}{\sqrt{e_2 e_3}}$  and  $S$  is the Frobenius norm of the Hessian matrix.  $\alpha$ ,  $\beta$  and  $\gamma$  control the sensitivity of the filter to  $R_A$ ,  $R_B$  and  $S$  measures.

**Sato line filter.** Similar to the work of Frangi et al. [5]. Sato et al. [16] proposed the following line filters to enhance tubular structures:

$$T(x) = \begin{cases} \exp(-\frac{e_1^2}{2(\alpha_1 e_c)^2}) & e_1 \leq 0 \text{ and } e_c \neq 0 \\ \exp(-\frac{e_1^2}{2(\alpha_2 e_c)^2}) & e_1 > 0 \text{ and } e_c \neq 0 \\ 0 & e_c = 0 \end{cases} \quad (6)$$

with  $e_c = \min(e_2, e_3)$ , and  $\alpha_1$  and  $\alpha_2$  are control parameters.

Scan	Image type	Spacing(mm)	Z-spacing (mm)	number of slices	kV/mAs
01	Angio-CT	0.76	1	355	120/40
02	Chest CT	0.71	0.7	415	140/74
03	Chest CT	0.62	0.7	534	120/77
04	LD Chest CT	0.86	1	426	100/44a
05	Chest CT	0.72	0.7	424	140/73

Table 1: Description of the first five CT scans of the *VESSEL12* challenge dataset. Angio-CT: CT with contrast agent, LD: Low Dose [15].

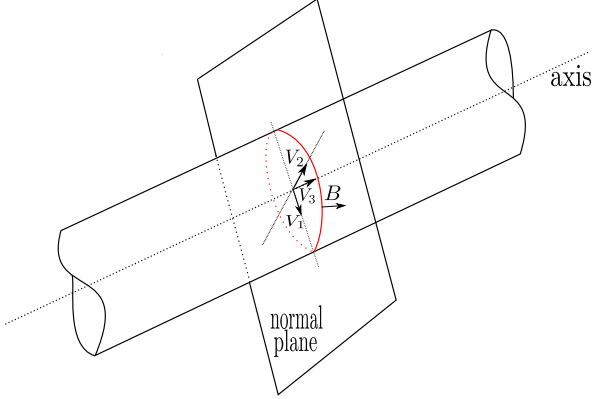


Figure 7: The medialness response obtained from the boundary information (red circle). The Cross-section plane of the tube is spanned by the eigenvectors  $v_1$  and  $v_2$  of the Hessian matrix [2].

**Krissian medialness filter.** Krissian et al. [10] proposed a medialness function which measures the degree to belong to the medial axis. The response function is estimated by measuring the boundary information at a circular neighborhood which radius is the used scale. The proposed medialness function is represented as follows:

$$R(X, \sigma, \theta) = \frac{1}{N} \sum_{i=0}^{N-1} |\nabla I^\sigma(X + \theta \sigma v_{\alpha_i})| \quad (7)$$

Here,  $X = (x, y, z)^T$  is a pixel point,  $I^\sigma(X)$  is the image at the scale  $\sigma$ ,  $N$  is the number of samples. The circle is defined by eigen vectors  $v_1$  and  $v_2$  and the radius  $r = \sigma\theta$ .

**Segmentation results.** We have used the pipeline of our algorithm to extract trees from the filtered data of each filter. We denote  $T_{RGF}$ ,  $T_{RGS}$ ,  $T_{RGK}$  respectively the tree obtained with region growing based on Frangi, Sato and krissian filter. We denote the TBT trees obtained by our method  $T_{RGTH}$ . Figure 10 summarize the detected airway trees ( $T_{RGF}$ ,  $T_{RGS}$ ,  $T_{RGK}$  and  $T_{RGTH}$ ) for each scan sorted by generation number (bronchi order). First order division corresponds to the trachea.

We illustrate also in Figure 8 the obtained tree for each algorithm. From Figure 10 and Figure 8 we can clearly notice that, for all of tested subjects, results obtained by our algorithm were significantly better than those



Figure 8: From left to right segmentation results of each algorithm:  $T_{RGTH}$ ,  $T_{RGF}$ ,  $T_{RGS}$ ,  $T_{RGK}$ .

obtained by other algorithms. Airway trees obtained using proposed segmentation algorithm were more expanded and contained more branches.

Moreover, the proposed method is robust in the sense that it yields good results on different types of scans (low-dose, CT with contrast agent and regular dose). Low-dose CT scans are increasingly utilized to quantify lung disease. In the fourth CT scan which is a Low-dose scan, our algorithm outperforms Frangi and Sato based region growing in terms of retrieved bronchi and Krissian based region growing in terms of generation number as well as detected bronchi.

In terms of runtime, Table 2 depicts the runtime in seconds of each algorithm performed on the first data set. We have used the same number of scales for all filters. Standard region growing algorithm is the fastest because it extracts at most 3 generations (30s). Our algorithm is ranked second with 840s and it is 2 minutes faster than the third one, the Frangi based region growing. The slowest algorithm is the Krissian based region growing.

### 4.3 Work in progress

In our current work, we are looking for increasing the number of detected generations and improving the rate of bronchi recognized per generation.

Tree	Time (in second)
$T_{RGTH}$	<b>840</b>
$T_{RGF}$	985
$T_{RGS}$	1020
$T_{RGK}$	1140

Table 2: Algorithms runtime.

Generation	Added bronchi
5th	4
6th	19
7th	12
8th	4

Table 3: Added bronchi per generation.

For this reason, we have analysed the Black Top-Hat response for each scale. We found that the region growing criterion excluded several bronchi improved by the filter. Excluded bronchi are those recognized by the three smaller scales but don't fill in the criterion range of the region growing. We calculated the BTH using the first three structural elements. The filter response for each SE is then thresholded and combined in a single volume. The obtained volume is added to the volume (see section 3.3) thresholded using the threshold employed in the second pass region growing. As illustrated in Figure 9, the segmentation is improved in terms of generation and in terms of number of retrieved bronchi. Table 3 presents the added bronchi at each generation in the second scan.

## 5 CONCLUSION AND PERSPECTIVES

In this article, we have presented a new approach based on 3D region growing to segment the bronchial tree. The algorithm is performed on the output of a multi-scale Black Top-Hat filter. It allows to highlight large as well as small bronchi while main bronchi and trachea are first extracted using a standard region growing. The proposed filter guides and constrains the growing process to identify airways region without leaking to the parenchyma region. The algorithm was tested using on different CT scan and it was compared to other region growing based methods using *vessel12* challenge data.

Experimental results show that our methods yields better results than those obtained by the four other methods in terms of the number of retrieved generation and runtime. Even if the method failed to extract bronchi after the seventh generation, our RG didn't leak into parenchyma and extract the TBT in few minutes. Therefore, it seems to be possible to complete the growing process with an advanced local tracking method on each bronchi which will be able to increase tree's depth. Future works will focus on the implementation of a complete segmentation pipeline in which the proposed method will be used as an initialization of the following extraction process.



Figure 9: Modified segmentation result in the first and second scan, added airways are marked in yellow.

## 6 REFERENCES

- [1] Deniz Aykac, Eric A Hoffman, Geoffrey McLennan, and Joseph M Reinhardt. Segmentation and analysis of the human airway tree from three-dimensional x-ray ct images. *Medical Imaging, IEEE Transactions on*, 22(8):940–950, 2003.
- [2] Christian Bauer and Homer Simpson. Segmentation of 3d tubular tree structures in medical images. 2010.
- [3] Edward Allen Boyden. *Segmental anatomy of the lungs: a study of the patterns of the segmental bronchi and related pulmonary vessels*. Blakiston Division, McGraw-Hill, 1955.
- [4] Anna Fabijańska. Two-pass region growing al-

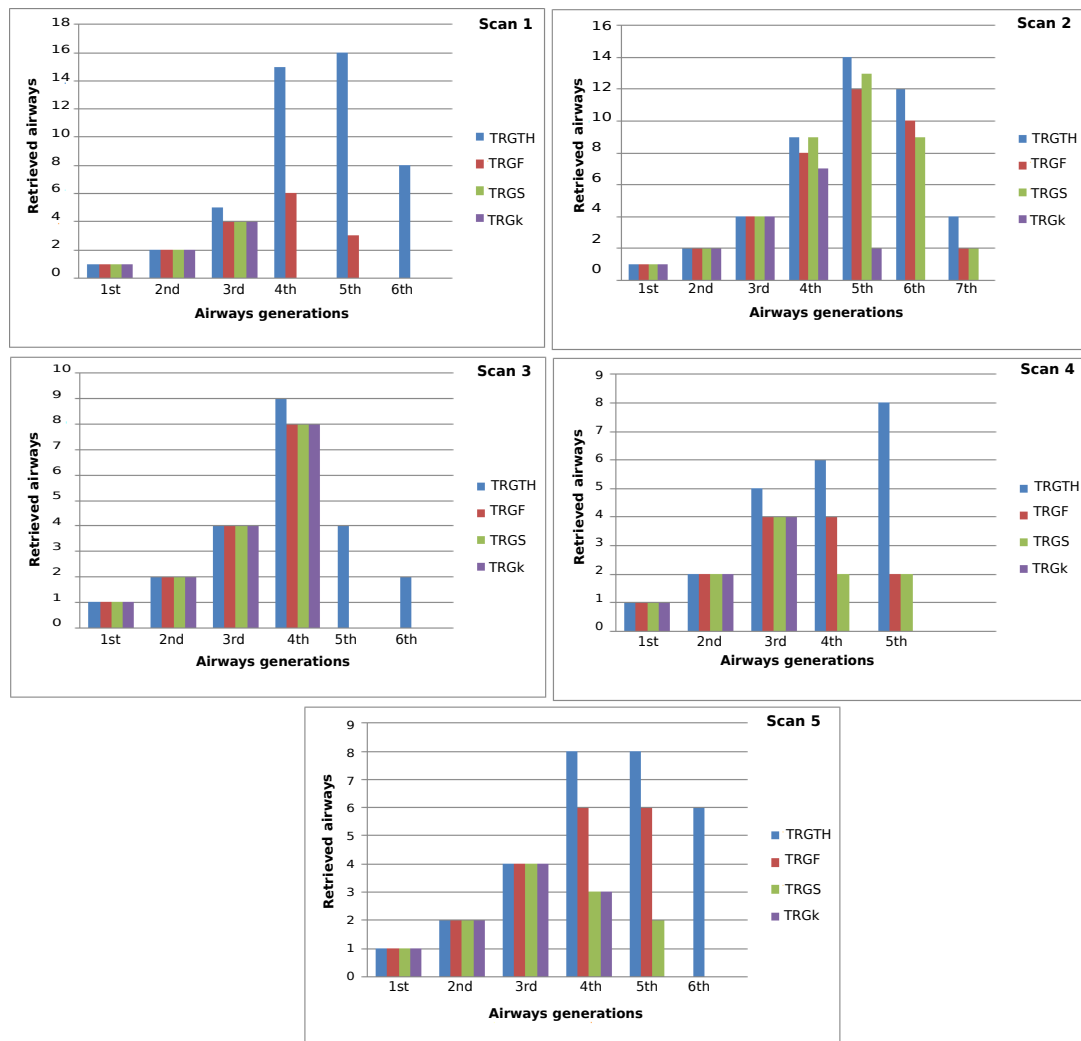


Figure 10: Number of detected airways sorted by generation number. The scan number is indicated on each histogram (cf. Table 1).

gorithm for segmenting airway tree from mdct chest scans. *Computerized Medical Imaging and Graphics*, 33(7):537–546, 2009.

[5] Alejandro F Frangi, Wiro J Niessen, Koen L Vincken, and Max A Viergever. Multiscale vessel enhancement filtering. In *Medical Image Computing and Computer-Assisted Intervention MICCAI98*, pages 130–137. Springer, 1998.

[6] Rafael C Gonzalez et al. Re woods, digital image processing. *Addison–Wesely Publishing Company*, 1992.

[7] Joris Heuberger, Antoine Geissbühler, and Henning Müller. Lung ct segmentation for image retrieval. *Medical Imaging and Telemedicine*, 2005.

[8] Shiyong Hu, Eric A Hoffman, and Joseph M Reinhardt. Automatic lung segmentation for accurate quantitation of volumetric x-ray ct images. *Medical Imaging, IEEE Transactions on*, 20(6):490–498, 2001.

[9] Benjamin Irving, Paul Taylor, and Andrew Todd-Pokropek. 3d segmentation of the airway tree using a morphology based method. In *Proceedings of 2nd international workshop on pulmonary image analysis*, pages 297–07, 2009.

[10] Karl Krissian, Grégoire Malandain, Nicholas Ayache, Régis Vaillant, and Yves Troussel. Model-based detection of tubular structures in 3d images. *Computer vision and image understanding*, 80(2):130–171, 2000.

[11] Jaesung Lee and Anthony P Reeves. Segmentation of the airway tree from chest ct using local volume of interest. In *Proc. of Second International Workshop on Pulmonary Image Analysis*, pages 273–284, 2009.

[12] Pechin Lo, Bram Van Ginneken, Joseph M Reinhardt, Tarunashree Yavarna, Pim A De Jong, Benjamin Irving, Catalin Fetita, Michael Ortner, Rô-

- mulo Pinho, Jan Sijbers, et al. Extraction of airways from ct (exact'09). *Medical Imaging, IEEE Transactions on*, 31(11):2093–2107, 2012.
- [13] Kensaku Mori, Jun-ichi Hasegawa, Jun-ichiro Toriwaki, Horfumi Anno, and Kazuhiro Katada. Recognition of bronchus in three-dimensional x-ray ct images with applications to virtualized bronchoscopy system. In *Pattern Recognition, 1996., Proceedings of the 13th International Conference on*, volume 3, pages 528–532. IEEE, 1996.
- [14] Chandrasekhar Pisupati, Lawrence Wolff, Elias Zerhouni, and Wayne Mitzner. Segmentation of 3d pulmonary trees using mathematical morphology. In *Mathematical morphology and its applications to image and signal processing*, pages 409–416. Springer, 1996.
- [15] Rina D Rudyanto, Sjoerd Kerkstra, Eva M Van Rikxoort, Catalin Fetita, Pierre-Yves Brillet, Christophe Lefevre, Wenzhe Xue, Xiangjun Zhu, Jianming Liang, İlkay Öksüz, et al. Comparing algorithms for automated vessel segmentation in computed tomography scans of the lung: the vessel12 study. *Medical image analysis*, 18(7):1217–1232, 2014.
- [16] Yoshinobu Sato, Shin Nakajima, Hideki Atsumi, Thomas Koller, Guido Gerig, Shigeyuki Yoshida, and Ron Kikinis. 3d multi-scale line filter for segmentation and visualization of curvilinear structures in medical images. In *CVRMed-MRCAS'97*, pages 213–222. Springer, 1997.
- [17] Milan Sonka, Wonkyu Park, and Eric A Hoffman. Rule-based detection of intrathoracic airway trees. *Medical Imaging, IEEE Transactions on*, 15(3):314–326, 1996.
- [18] Ronald M Summers, David H Feng, Steven M Holland, Michael C Sneller, and James H Shelhamer. Virtual bronchoscopy: segmentation method for real-time display. *Radiology*, 200(3):857–862, 1996.
- [19] Oliver Weinheimer, Tobias Achenbach, and Christoph Düber. Fully automated extraction of airways from ct scans based on self-adapting region growing. *Computerized Tomography*, 27(1):64–74, 2008.